IV. Positional and equivalent isotropic thermal parameters are given in Table VIII, and selected bond distances and angles are collected in Table VII.

Supplementary Material Available: Listings of thermal parameters for non-hydrogen atoms, all bond distances and angles, and positional and isotropic thermal parameters for hydrogen atoms of **10** and **17a**$\cdot C_7H_8$ (12 pages); listings of observed and calculated structure factors (68 pages). Ordering information is given on any current masthead page.

Synthesis and Coordination Chemistry of a New Class of Binucleating Ligands: Pyridyl-Substituted Diphosphines

Peter H. M. Budzelaar* and John H. G. Frijns

Koninklijke/Shell-Laboratorium, Amsterdam (Shell Research B.V.), Postbus 3003,
1003 AA Amsterdam, The Netherlands

A. Guy Orpen

School of Chemistry, The University of Bristol, Cantock's Close, BS8 1TS U.K.

Received September 29, 1989

The syntheses of three new binucleating ligands, $(C_6H_5)(2\text{-}C_5H_4N)P(CH_2)_nP(C_6H_5)(2\text{-}C_5H_4N)$ (n = 1, DPyPM; n = 2, DPyPE; n = 3, DPyPP), are described and their coordination properties have been probed. *rac*-DPyPM reacts with $[Rh(CO)_2Cl]_2$ to produce a binuclear complex DPyPM$[Rh(CO)Cl]_2$, in which the ligand forms three bridges between the two Rh(CO)Cl fragments. The structure of the bis(acetonitrile) solvate (determined by X-ray diffraction) shows two approximately square-planar rhodium centers with a (nonbonded) Rh–Rh distance of 3.093 (1) Å. The meso isomers of DPyPE and DPyPP react with $[Rh(CO)_2Cl]_2$ to give $[L_2Rh_2Cl_2][Rh(CO)_2Cl_2]_2$; the structure of the DPyPP complex was determined by X-ray crystallography. In the complex cation, each rhodium atom is surrounded in an octahedral fashion by two phosphorus atoms of one DPyPP ligand, two pyridyl nitrogens of the second DPyPP, the second rhodium atom (Rh–Rh = 2.651 (3) Å), and a chlorine atom trans to Rh.

Introduction

Bimetallic complexes are, among other reasons, interesting for their potential applications in catalysis. Homobimetallic complexes can bind to unsaturated substrates in ways that are not possible for their monometallic analogues and thus can lead to new substrate reactivity. Heterobimetallic complexes could give rise to "tandem" reactions; "early–late" bimetallic complexes have received a great deal of attention in recent years, primarily because of their ability to bind and (through polarization) activate oxygen-containing substrates.[1]

One approach to the synthesis of bimetallic complexes is the use of binucleating ligands, two of the more popular classes being diphosphinomethanes and pyridylphosphines.[2] Both of these ligands tend to form complexes in which two metal atoms are surrounded by two ligand molecules in a "trans" fashion. Because of the asymmetry of the pyridylphosphine ligand, two types of M_2L_2 complexes may be formed, "head-to-tail" and "head-to-head". The large difference in donor properties between the "hard" nitrogen and the "soft" phosphorus causes a preference for formation of "head-to-head" complexes in early–late mixed-metal systems; in homobimetallic systems, the "head-to-tail" arrangement is generally observed. Regardless of the arrangement of the metals and donor atoms in such complexes, their geometries are not very favorable for the occurrence of "real" bimetallic reactions (in which both metals participate simultaneously). The space between the metal atoms can sometimes be used to trap a small substrate molecule (CO, SO_2, Cl^-), but apart from that the sites available for reactions are rather far apart, as illustrated below. Complexes with the two ligand molecules in a "cis" orientation could be more interesting. However, few such complexes are known, and none are expected to retain their geometry once open sites have been created for reactions.

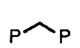

diphosphinomethane

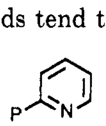

pyridylphosphine

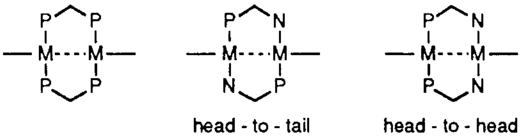

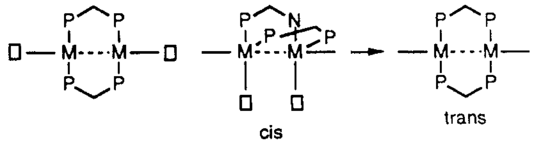

We decided to develop a series of ligands that would have a natural preference for the "cis" arrangement shown

---

[1] See, e.g.: Roberts, D. A.; Geoffroy, G. L. Compounds with Heteronuclear Bonds between Transition Metals. In *Comprehensive Organometallic Chemistry*; Wilkinson, G., Ed.; Pergamon: New York, 1982; Vol. 6, pp 763ff.

[2] Puddephat, R. J. *Chem. Soc. Rev.* **1983**, *12*, 99. Balch, A. L. In *Homogeneous Catalysis with Metal Phosphine Complexes*; Pignolet, L. H., Ed.; Plenum: New York, 1983; pp 167ff.

0276-7333/90/2309-1222$02.50/0

Scheme I. Synthesis of Pyridyl-Substituted Diphosphines

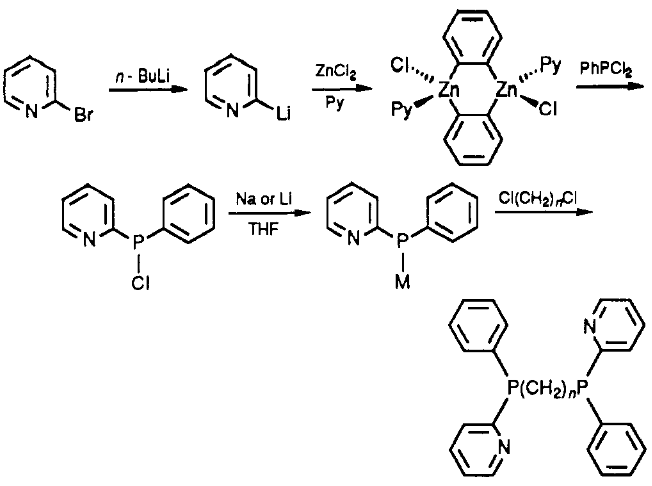

above by linking two binucleating pyridylphosphine ligand units with an aliphatic chain:

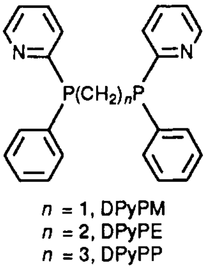

The meso forms of DPyPE and DPyPP should prefer coordination geometries as shown in A; these ligands

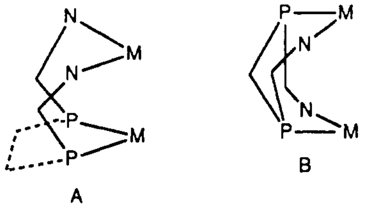

should also be suitable for the preparation of early–late heterobimetallic complexes. Although similar P,P chelates are also possible with *meso*-DPyPM, the *rac* form of this ligand is expected to prefer a different "flyover" geometry, as illustrated in B. The syntheses of the three new ligands and our first investigations into their coordination properties are described in this work.

Results and Discussion

Ligand Synthesis. The synthesis of the ligands DPyPM–DPyPP is outlined in Scheme I. The use of the pyridylzinc intermediate is necessary because direct reaction of organolithium reagents with $PhPCl_2$ usually yields a mixture of $PhPR_2$, PhP(R)Cl, and $PhPCl_2$;[3] the zinc method was also used by Kyba in the synthesis of asymmetric *o*-phenylenediphosphine ligands.[4] Reduction of PhP(Py)Cl with sodium is capricious and may take from a few hours to several weeks in refluxing THF; addition of a small amount of 4,4'-di-*tert*-butylbiphenyl sometimes helps. The reduction with activated lithium is much quicker but produces a somewhat less pure product. The final coupling reaction with ethylene chloride and propylene chloride proceeds cleanly, but the reaction with methylene chloride produces considerable amounts of $PhP(Py)CH_3$, $PhP(Py)CH_2Cl$, and $(PhPPy)_2$ as byproducts; column chromatography finally gives a pure product in moderate yield. All three ligands were obtained as approximately equimolar mixtures of *meso* and *rac* forms;

Table I. NMR Data (δ_C, ppm (J_{PC}, Hz)) for Pyridyldiphosphine Ligands ($CDCl_3$)

	ligand		
	DPyPM	DPyPE	DPyPP
C_i	137.5 (7)	136.6 (13)	137.0 (13)
C_o	133.8 (21)	133.6 (20)	133.7 (20)
C_m	128.2 (8)	128.3 (7)	128.4 (7)
C_p	129.0	129.0	129.1
C_2	164.3 (2)	164.6	165.1 (2)
C_3	128.3 (30)	127.5 (24)	127.6 (24)
C_4	134.9 (7)	135.0 (5)	135.1 (5)
C_5	121.9	121.8	121.8
C_6	149.8 (7)	149.8 (8)	149.9 (8)
CH_2	24.6 (19)	23.2 (18, 22)	28.8 (13, 11; α), 22.5 (18; β)
	δ_P, ppm (J_{PP}, Hz[a])		
	−19.2 (>30)	−10.4 (≈35)	−14.5 (<1)

[a] Determined from the ^{13}C NMR spectrum.

Table II. NMR Data (δ_C, ppm (J_{PC}, Hz; J_{RhC}, Hz)) for *rac*-DPyPM[Rh(CO)Cl]$_2$ and [(*meso*-DPyPE)$_2$Rh$_2$Cl$_2$][Rh(CO)$_2$Cl$_2$]$_2$

	complex	
	DPyPM[Rh(CO)Cl]$_2$ (DMSO-d_6)	[(DPyPE)$_2$Rh$_2$Cl$_2$]-[Rh(CO)$_2$Cl$_2$]$_2$ (CD_3OD/CD_3CN)
C_i	127.6 (46, 13; 2)	127.7 (56)
C_o	134.5[b]	133.8 (10)
C_m	129.4[b]	129.9 (11)
C_p	132.8	133.4
C_2	161.0 (70, −3)	165.0 (69)
C_3	124.7	133.0 (10)
C_4	138.8	140.5
C_5	124.7	130.4
C_6	155.9[b]	155.3 (13)
CH_2	15.4 (23)	30.0 (38, 7)
CO	189.1 (18; 70)	182.8 (–; 71)
	δ_P, ppm ($^1J_{RhP}$, Hz)	
	36.9 (161[a])	24.0 (≈112)

[a] $^3J_{RhP} = 9$ Hz, $^2J_{PP} = 67$ Hz; $J_{RhRh} < 2$ Hz. [b] Unresolved multiplet.

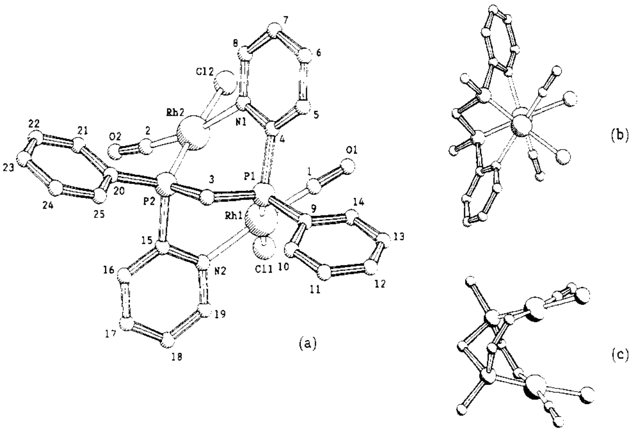

Figure 1. PLUTO drawings of DPyPM[Rh(CO)Cl]$_2$. All hydrogen atoms have been omitted; in parts b and c, some phenyl and pyridyl carbons have been omitted as well.

---

[3] Sasse, K. Organische Phosphorverbindungen. In *Methoden der Organische Chemie* (*Houben*-Weyl); Georg Thieme: Stuttgart, 1963; Vol. XII/1, pp 203ff. Kleiner, H.-J. Phosphinigsäure und deren Derivate. In *Methoden der Organische Chemie* (*Houben-Weyl*); Georg Thieme, Stuttgart, 1982; Vol. E1, pp 246ff.

[4] Kyba, E. P.; Kerby, M. C.; Rines, S. P. *Organometallics* **1986**, *5*, 1189. See also: Jore, D.; Guillerm, D.; Chodkiewicz, W. *J. Organomet. Chem.* **1978**, *149*, C7.

separation was not attempted. NMR data are collected in Table I.

Reaction of DPyPM with $[Rh(CO)_2Cl]_2$. Addition of a solution of DPyPM to $[Rh(CO)_2Cl]_2$ produces a precipitate of dark *rac*-DPyPM[Rh(CO)Cl]$_2$ (1); any complexes derived from *meso*-DPyPM remain in solution and were not characterized. Complex 1 is virtually insoluble in most organic solvents (benzene, THF, CH_2Cl_2). It dissolves quickly in acetonitrile but then largely reprecipitates again as the bis(acetonitrile) solvate; the solvent of crystallization is easily removed again in vacuo. It also dissolves in highly polar solvents such as pyridine and DMSO; NMR data for the DMSO solution are given in Table II. Detailed analysis of the ^{13}C and ^{31}P NMR spectra allowed the determination of the P–P, Rh–P, and Rh–Rh coupling constants; all of these data agree with a structure of type B, except that the Rh–Rh coupling constant is rather small. To unambiguously establish the proposed structure of the complex, we carried out an X-ray determination on $1 \cdot 2CH_3CN$.

X-ray Structure of *rac*-DPyPM[Rh(CO)Cl]$_2$·2CH$_3$CN (1). The structure consists of discrete DPyPM-[Rh(CO)Cl]$_2$ molecules (Figure 1) and molecules of acetonitrile of crystallization, with no MeCN···Rh interactions apparent. The rhodium complex contains two square-planar-surrounded Rh atoms having P cis to CO, as expected. The ligand arrangements around the Rh atoms are nearly staggered, as is evident from the projection along the Rh–Rh vector (Figure 1b). Also, the coordination planes are not parallel, but are inclined at an angle of 34°, leaving a "hole" which is clearly illustrated in Figure 1c. The Rh–Rh distance (3.09 Å) is too large for a direct metal–metal bond. However, molecular models indicate that the molecular skeleton should be able to "breathe", i.e., the Rh–Rh distance can be varied in the range 2.5–4 Å without introducing undue strain in the rest of the molecule. The structure of this complex is clearly of type B and illustrates the hoped-for cis coordination of the linked pyridylphoshine units.

Reactions of DPyPE and DPyPP with $[Rh(CO)_2Cl]_2$. Addition of a THF solution of DPyPE or DPyPP to a THF suspension of $[Rh(CO)_2Cl]_2$ results in a color change from yellow to deep red and in the slow formation of a red precipitate. This precipitate is poorly soluble in most solvents; the solubility in methanol/acetonitrile mixtures is high enough to allow NMR measurements, although the quality of the spectra is not very good. The ^1H NMR spectra of both products show a characteristic low-field resonance for the α-pyridyl protons (L = DPyPE, 9.6 ppm; L = DPyPP, 10.3 ppm), indicating coordination of the pyridyl groups to rhodium. The ^{31}P NMR spectra show a "doublet" (with splittings of 118 Hz for DPyPE and 112 Hz for DPyPP) with some unresolved fine structure. Most of the resonances in the ^{13}C NMR spectrum of the DPyPE complex (Table II) are complex and indicate (virtual) coupling to several rhodium and/or phosphorus atoms. The infrared spectrum of the DPyPP complex shows two CO stretch vibrations, at 1982 and 2062 cm^{-1} (Nujol mull); the elemental analysis produced the stoichiometry [DPyPP]$Rh_2(CO)_2Cl_3$. Since it was not easy to deduce a plausible structure from these data, we decided to determine the structure by X-ray diffraction. Suitable crystals of the DPyPP complex were grown by crystallization from hot benzonitrile.

X-ray Structure of [(*meso*-DPyPP)$_2$Rh$_2$Cl$_2$][Rh(CO)$_2$Cl$_2$]$_2$ (2). The structure of the DPyPP complex consists of discrete ions [(*meso*-DPyPP)$_2Rh_2Cl_2]^{2+}$ and *cis*-$[Rh(CO)_2Cl_2]^-$; apparently, only the products formed from the meso isomers of DPyPE and DPyPP precipitate under the reaction conditions. Several compounds containing the rhodium carbonyl anion have been reported before;[5] the geometry in the present complex is normal. The cation (Figure 2), which has crystallographic $P\bar{1}$ (C_i) symmetry, consists of a quadruply bridged Rh_2^{4+} unit containing a single Rh–Rh bond; this structural unit is well-known from carboxylato complexes.[6] Each rhodium atom is coordinated by two phosphorus atoms of one DPyPP ligand and two pyridyl nitrogens of the other ligand in the euqatorial positions; two axial chlorines complete the octahedral environments of the rhodium atoms. The Rh–Rh distance (2.65 Å) is normal for Rh(II)–Rh(II) singly bonded dimers[6] and is close to the P···N distances in the DPyPP ligand (2.74 Å), reflecting the good match between donor and acceptor geometries. The coordination mode of each DPyPP ligand closely resembles the structural type A mentioned in the Introduction and once again demonstrates the tendency toward cis coordination of the pyridylphosphine units. However, it appears that any (DPyPP)Rh_2 units formed initially from DPyPP and $[Rh(CO)_2Cl]_2$ are more reactive toward a second molecule of DPyPP than the starting material; this results in formation of (DPyPP)$_2Rh_2$ units which lack the open sites necessary for bimetallic reactivity.

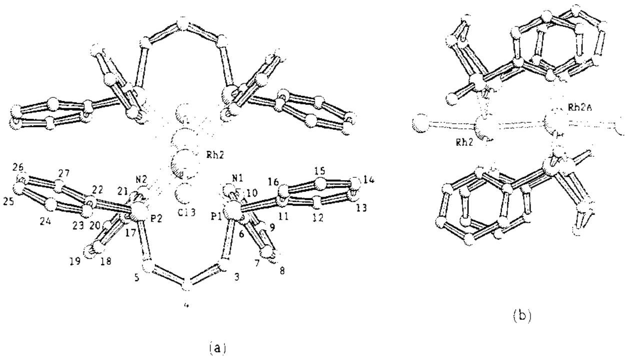

Figure 2. PLUTO drawing of the (*meso*-DPyPP)$_2Rh_2Cl_2^{2+}$ dication. Hydrogen atoms are not shown; in part b, most phenyl carbons have been omitted for clarity as well.

Conclusions

Judging from the structures of rhodium complexes 1 and 2, the pyridyl-substituted diphosphines described in this work do indeed give rise to bimetallic systems containing two cis-coordinated pyridylphosphine units. Whether this will also result in a greater or different reactivity (compared with the more usual trans systems) remains to be investigated. Of the complexes studied, the DPyPM complex 1 is the most interesting because the CO and/or the Cl ligands could possibly be removed, leaving an "open-faced" bimetallic system.

Experimental Section

Ligand Syntheses. General Remarks. All reactions were carried out under an Ar or N_2 atmosphere. Solvents were distilled from Na (toluene or hexane) or Na/benzophenone (ether, THF) prior to use; pyridine was distilled from calcium hydride. All commercially available chemicals were used as received. ^1H, ^{13}C, and ^{31}P NMR spectra were recorded on a Bruker WH-250 or Varian XL-200 or VXR-300 instrument.

Phenyl(2-pyridyl)chlorophosphine. "Anhydrous" $ZnCl_2$ (47 g, 0.35 mol) was molten in vacuo, cooled to room temperature, and dissolved in 100 mL of diethyl ether. A mixture of 200 mL of diethyl ether and 216 mL (0.35 mol) of a 1.6 M *n*-butyllithium

---

[5] See, e.g.: Mantovani, A.; Pelloso, M.; Bandoli, G.; Crociani, B. *J. Chem. Soc., Dalton Trans.* **1984**, 2223, and references cited therein.

[6] See, e.g.: Felthouse, T. R. *Prog. Inorg. Chem.* **1982**, *29*, 73, and references cited therein.

Table III. Crystallographic Data for Compounds 1 and 2

	$1{\cdot}2CH_3CN$	2
formula	$C_{29}H_{26}Cl_2N_4O_2P_2Rh_2$	$C_{54}H_{48}Cl_6N_4O_4P_4Rh_4$
formula weight	801.22	1565.2
space group	$P2_1/c$	$P2_1/n$
a, Å	14.468 (4)	12.031 (2)
b, Å	15.085 (5)	20.666 (3)
c, Å	15.618 (4)	13.077 (2)
β, deg	108.26 (2)	115.92 (2)
V, Å^3	3237 (2)	2924.5 (8)
Z	4	2
d_{calc}, g/cm^3	1.64	1.75
cryst size, mm	0.85 × 0.5 × 0.36	0.5 × 0.2 × 0.1
μ (Mo Kα), cm^{-1}	13.0	15.24
orient reflcns (no.; range)	25; $30 < 2\vartheta < 32°$	25; $25 < 2\vartheta < 27°$
scan method	$\vartheta/2\vartheta$	ω, Wyckoff
data coll range	$4 < 2\vartheta < 45°$	$4 < 2\vartheta < 50°$
decay, %	18	−2
total unique	4252	5155
total obsd	3630 ($I > 2\sigma(I)$)	3167 ($I > 2\sigma(I)$)
refined params	373	343
transm factors	0.717–0.426	0.82–0.68
R^a	0.044	0.052
$R_w{}^b$	0.045	0.050
g(weights)^c	0.0008	0.0005
quality-of-fit S^d	1.56	1.05
res peaks, e/Å^3	1.8	0.8

[a] R v $\sum|\Delta|/\sum|F_o|$, $\Delta = |F_o| - |F_c|$. [b] $R_w = \sum w^{1/2}|\Delta|/\sum w^{1/2}|F_o|$. [c] $w = [\sigma_c{}^2(F_o) + gF_o{}^2]^{-1}$. [d] $S = [\sum w\Delta^2/(N_{obs} - N_{par})]^{1/2}$.

Table IV. Positional and Equivalent Isotropic Thermal Parameters for $1\bullet 2CH_3CCN$

atom	x	y	z	U_{eq},^{a} Å^2
Rh(1)	0.15333 (3)	0.16913 (3)	0.36229 (3)	0.0340 (2)
Rh(2)	0.34587 (3)	0.27421 (3)	0.40311 (3)	0.0364 (2)
Cl(1)	0.0746 (1)	0.1760 (1)	0.2029 (1)	0.0542 (5)
Cl(2)	0.4182 (1)	0.2029 (1)	0.3041 (1)	0.0650 (6)
P(1)	0.2217 (1)	0.15476 (9)	0.50960 (9)	0.0345 (4)
P(2)	0.2677 (1)	0.33803 (9)	0.4884 (1)	0.0365 (5)
O(1)	0.2240 (4)	−0.0082 (3)	0.3353 (3)	0.083 (2)
O(2)	0.3177 (4)	0.4318 (4)	0.2865 (3)	0.088 (2)
N(1)	0.4019 (3)	0.1691 (3)	0.4980 (3)	0.040 (2)
N(2)	0.0895 (3)	0.2931 (3)	0.3782 (3)	0.040 (2)
C(1)	0.1977 (4)	0.0610 (4)	0.3468 (4)	0.049 (2)
C(2)	0.3237 (5)	0.3702 (4)	0.3302 (4)	0.053 (2)
C(3)	0.2419 (4)	0.2614 (3)	0.5697 (3)	0.038 (2)
C(4)	0.3494 (4)	0.1193 (4)	0.5403 (3)	0.039 (2)
C(5)	0.3910 (5)	0.0534 (4)	0.5989 (4)	0.052 (2)
C(6)	0.4901 (5)	0.0364 (5)	0.6194 (4)	0.063 (3)
C(7)	0.5428 (5)	0.0881 (5)	0.5795 (5)	0.065 (3)
C(8)	0.4979 (4)	0.1520 (4)	0.5194 (4)	0.055 (2)
C(9)	0.1646 (4)	0.0805 (4)	0.5685 (4)	0.042 (2)
C(10)	0.1237 (5)	0.1124 (4)	0.6324 (5)	0.064 (3)
C(11)	0.0759 (6)	0.0542 (5)	0.6721 (6)	0.088 (3)
C(12)	0.0690 (6)	−0.0338 (5)	0.6526 (5)	0.069 (3)
C(13)	0.1069 (7)	−0.0638 (5)	0.5896 (6)	0.093 (4)
C(14)	0.1552 (6)	−0.0084 (4)	0.5462 (5)	0.075 (3)
C(15)	0.1392 (4)	0.3635 (3)	0.4245 (4)	0.040 (2)
C(16)	0.0957 (5)	0.4436 (4)	0.4269 (4)	0.050 (2)
C(17)	−0.0025 (5)	0.4528 (4)	0.3831 (4)	0.061 (2)
C(18)	−0.0546 (5)	0.3816 (4)	0.3381 (4)	0.056 (2)
C(19)	−0.0070 (4)	0.3027 (4)	0.3368 (4)	0.050 (2)
C(20)	0.3117 (4)	0.4395 (4)	0.5492 (4)	0.042 (2)
C(21)	0.3760 (5)	0.4940 (4)	0.5224 (4)	0.059 (3)
C(22)	0.4088 (5)	0.5714 (4)	0.5661 (5)	0.069 (3)
C(23)	0.3828 (5)	0.5973 (4)	0.6391 (5)	0.063 (3)
C(24)	0.3211 (5)	0.5443 (4)	0.6680 (4)	0.058 (3)
C(25)	0.2865 (5)	0.4650 (4)	0.6251 (4)	0.050 (2)
N(3)	0.707 (1)	0.1809 (9)	0.479 (1)	0.206 (9)
C(26)	0.769 (1)	0.231 (1)	0.510 (1)	0.150 (8)
C(27)	0.841 (1)	0.296 (1)	0.540 (1)	0.30 (1)
N(4)	0.7500 (9)	0.2489 (9)	0.230 (1)	0.195 (7)
C(28)	0.687 (1)	0.2058 (8)	0.2228 (9)	0.119 (6)
C(29)	0.600 (1)	0.1527 (7)	0.201 (1)	0.164 (8)

[a] Equivalent isotropic U, defined as one-third of the trace of the orthogonalized $\mathbf{U}_{ij}$ tensor.

Table V. Selected Bond Lengths and Angles for $1\bullet 2CH_3CCN$

Bond Distances, Å

Rh(1)–Rh(2)	3.093 (1)	Rh(1)–Cl(1)	2.393 (2)	Rh(1)–P(1)	2.212 (2)
Rh(1)–C(1)	1.797 (6)	Rh(2)–Cl(2)	2.379 (2)	Rh(2)–P(2)	2.219 (2)
Rh(2)–C(2)	1.808 (6)	P(1)–C(3)	1.839 (5)	P(1)–C(4)	1.837 (6)
P(2)—C(3)	1.839 (5)	P(2)–C(15)	1.854 (6)	P(2)–C(20)	1.808 (6)
O(2)–C(2)	1.140 (8)	N(1)–C(4)	1.376 (7)	N(1)–C(8)	1.348 (8)
N(2)–C(19)	1.350 (8)	C(4)–C(5)	1.358 (8)	C(5)–C(6)	1.39 (1)
C(7)–C(8)	1.360 (9)	C(15)–C(16)	1.368 (8)	C(18)–C(19)	1.378 (9)
C(16)–C(17)	1.38 (1)	C(17)–C(18)	1.373 (9)	N(2)–C(15)	1.357 (7)
Rh(1)–N(2)	2.134 (5)	P(1)–C(9)	1.806 (6)	C(6)–C(7)	1.37 (1)
Rh(2)–N(1)	2.148 (5)	O(1)–C(1)	1.144 (8)		

Bond Angles, deg

Rh(2)–Rh(1)–Cl(1)	107.26 (5)	Rh(2)–Rh(1)–P(1)	75.84 (5)
Rh(2)–Rh(1)–C(1)	99.0 (2)	Cl(1)–Rh(1)–P(1)	176.46 (8)
Cl(1)–Rh(1)–C(1)	88.5 (2)	P(1)–Rh(1)–N(2)	91.9 (1)
N(2)–Rh(1)–C(1)	175.5 (2)	Rh(1)–Rh(2)–Cl(2)	100.69 (5)
Rh(1)–Rh(2)–N(1)	83.4 (1)	Rh(1)–Rh(2)–C(2)	108.1 (2)
Cl(2)–Rh(2)–N(1)	88.1 (1)	Cl(2)–Rh(2)–C(2)	88.9 (2)
P(2)–Rh(2)–C(2)	90.4 (2)	N(1)–Rh(2)–C(2)	168.5 (2)
Rh(1)–P(1)–C(4)	112.7 (2)	Rh(2)–P(2)–C(15)	112.3 (2)
Rh(2)–N(1)–C(8)	116.7 (4)	C(4)–N(1)–C(8)	117.2 (5)
Rh(1)–N(2)–C(19)	117.3 (4)	C(15)–N(2)–C(19)	117.8 (5)
Rh(2)–C(2)–O(2)	174.4 (7)	P(1)–C(3)–P(2)	103.4 (2)
P(1)–C(4)–C(5)	125.9 (5)	N(1)–C(4)–C(5)	121.9 (6)
C(5)–C(6)–C(7)	118.1 (6)	C(6)–C(7)–C(8)	120.3 (7)
P(2)–C(15)–N(2)	113.5 (4)	N(2)–C(15)–C(16)	122.3 (6)
P(2)–C(15)–C(16)	124.1 (4)	C(17)–C(18)–C(19)	119.1 (6)
C(16)–C(17)–C(18)	119.4 (6)	Rh(2)–P(2)–C(3)	113.2 (2)
Rh(2)–Rh(1)–N(2)	85.5 (1)	C(3)–P(2)–C(15)	96.6 (3)
Cl(1)–Rh(1)–N(2)	90.0 (1)	Rh(2)–N(1)–C(4)	126.1 (4)
P(1)–Rh(1)–C(1)	89.4 (2)	Rh(1)–N(2)–C(15)	124.8 (4)
Rh(1)–Rh(2)–P(2)	75.56 (5)	Rh(1)–C(1)–O(1)	178.4 (6)
Cl(2)–Rh(2)–P(2)	175.76 (8)	P(1)–C(4)–N(1)	112.2 (4)
P(2)–Rh(2)–N(1)	93.4 (1)	C(4)–C(5)–C(6)	119.8 (6)
Rh(1)–P(1)–C(3)	113.1 (2)	N(1)–C(8)–C(7)	122.6 (6)
C(3)–P(1)–C(4)	97.8 (3)	C(15)–C(16)–C(17)	119.2 (6)
C(2)–C(19)–C(18)	122.1 (6)		

Table VI. Positional and Equivalent Isotropic Thermal Parameters for 2

atom	x	y	z	U_{eq}, Å^2
Rh(1)	0.22915 (7)	0.20071 (4)	0.28477 (6)	0.0625 (3)
Cl(1)	0.1778 (3)	0.1037 (2)	0.3452 (3)	0.120 (2)
Cl(2)	0.0234 (3)	0.2174 (2)	0.1551 (3)	0.116 (2)
O(1)	0.3067 (9)	0.3250 (5)	0.227 (1)	0.154 (5)
O(2)	0.4893 (8)	0.1764 (4)	0.4417 (8)	0.120 (4)
C(1)	0.274 (1)	0.2770 (6)	0.245 (1)	0.094 (5)
C(2)	0.388 (1)	0.1863 (5)	0.3807 (9)	0.073 (4)
Rh(2)	0.47394 (6)	0.05250 (3)	0.04359 (5)	0.0434 (2)
Cl(3)	0.4443 (2)	0.1590 (1)	0.1209 (2)	0.0607 (8)
P(1)	0.6767 (2)	0.0739 (1)	0.1375 (2)	0.0511 (8)
P(2)	0.4632 (2)	0.1092 (1)	−0.1083 (2)	0.0465 (7)
N(1)	0.2765 (5)	0.0303 (3)	−0.0329 (5)	0.049 (2)
N(2)	0.4707 (6)	−0.0004 (3)	0.1876 (5)	0.051 (2)
C(3)	0.7300 (8)	0.1535 (4)	0.1174 (7)	0.060 (3)
C(4)	0.6954 (8)	0.1713 (5)	−0.0069 (8)	0.070 (4)
C(5)	0.5566 (8)	0.1835 (4)	−0.0755 (7)	0.056 (3)
C(6)	0.7763 (7)	0.0184 (4)	0.1063 (7)	0.052 (3)
C(7)	0.9024 (8)	0.0274 (5)	0.1540 (8)	0.068 (4)
C(8)	0.977 (1)	−0.0117 (6)	0.1289 (9)	0.079 (4)
C(9)	0.9244 (9)	−0.0610 (5)	0.0515 (9)	0.071 (4)
C(10)	0.2026 (8)	0.0678 (4)	−0.0063 (8)	0.064 (4)
C(11)	0.7372 (8)	0.0705 (4)	0.2927 (7)	0.057 (3)
C(12)	0.8035 (9)	0.0193 (5)	0.3539 (8)	0.067 (4)
C(13)	0.847 (1)	0.0179 (6)	0.4720 (9)	0.087 (4)
C(14)	0.826 (1)	0.0686 (6)	0.5256 (9)	0.087 (4)
C(15)	0.760 (1)	0.1207 (6)	0.4652 (8)	0.094 (5)
C(16)	0.7151 (9)	0.1213 (5)	0.3497 (8)	0.080 (4)
C(17)	0.5157 (7)	0.0650 (4)	−0.1989 (7)	0.048 (3)
C(18)	0.5388 (8)	0.0973 (4)	−0.2801 (7)	0.062 (3)
C(19)	0.5773 (9)	0.0633 (5)	−0.3505 (8)	0.074 (4)
C(20)	0.588 (1)	−0.0018 (5)	−0.3402 (8)	0.072 (4)
C(21)	0.436 (1)	0.0316 (4)	0.2578 (7)	0.070 (4)
C(22)	0.3110 (8)	0.1397 (4)	−0.2059 (7)	0.054 (3)
C(23)	0.2424 (9)	0.1737 (4)	−0.1608 (9)	0.070 (4)
C(24)	0.128 (1)	0.1985 (5)	−0.231 (1)	0.089 (5)
C(25)	0.0789 (9)	0.1879 (5)	−0.346 (1)	0.082 (4)
C(26)	0.147 (1)	0.1579 (5)	−0.3931 (9)	0.087 (4)
C(27)	0.2609 (8)	0.1335 (4)	−0.3221 (8)	0.067 (3)

Table VII. Selected Bond Lengths and Angles for 2[a]

Bond Distances, Å

Rh(1)–Cl(1)	2.336 (4)	Rh(1)–Cl(2)	2.335 (4)	Rh(1)–C(1)	1.81 (1)
O(1)–C(1)	1.13 (2)	O(2)–C(2)	1.15 (2)	Rh(1)–C(2)	1.79 (1)
Rh(2)–Cl(3)	2.511 (2)	Rh(2)–P(1)	2.244 (3)	Rh(2)–P(2)	2.261 (2)
Rh(2)–N2)	2.193 (6)	Rh(2)–Rh(2A)	2.650 (1)	P(1)–C(3)	1.826 (9)
P(1)–C(11)	1.834 (9)	P(2)–C(5)	1.839 (9)	P(2)–C(17)	1.814 (9)
N(1)–C(10)	1.34 (1)	N(1)–C(6A)	1.34 (1)	N(2)–C(21)	1.34 (1)
C(3)–C(4)	1.54 (1)	C(4)–C(5)	1.53 (1)	C(6)–C(7)	1.38 (1)
C(8)–C(9)	1.38 (2)	C(9)–C(10A)	1.38 (2)	C(20)–C(21A)	1.38 (1)
C(17)–C(18)	1.38 (1)	C(18)–C(19)	1.39 (1)	C(19)–C(20)	1.35 (2)
Rh(2)–N(1)	2.185 (7)	P(2)–C(22)	1.83 (1)	C(7)–C(8)	1.35 (2)
P(1)–C(6)	1.829 (9)	N(2)–C(17A)	1.35 (1)		

Bond Angles

Cl(1)–Rh(1)–Cl(2)	91.1 (1)	Cl(1)–Rh(1)–C(1)	177.2 (4)
Cl(2)–Rh(1)–C(1)	90.9 (5)	Cl(2)–Rh(1)–C(2)	178.1 (3)
Rh(1)–C(1)–O(1)	176.0 (1)	Rh(1)–C(2)–O(2)	179.0 (1)
Cl(3)–Rh(2)–P(1)	85.34 (9)	Cl(3)–Rh(2)–P(2)	86.29 (8)
Cl(3)–Rh(2)–N(2)	91.9 (2)	Cl(3)–Rh(2)–Rh(2A)	172.90 (8)
P(1)–Rh(2)–N(1)	174.8 (2)	P(1)–Rh(2)–N(2)	92.9 (2)
P(2)–Rh(2)–N(1)	94.2 (2)	P(2)–Rh(2)–N(2)	175.9 (2)
N(1)–Rh(2)–N(2)	82.2 (2)	N(1)–Rh(2)–Rh(2A)	92.6 (2)
Rh(2)–P(1)–C(3)	117.7 (3)	Rh(2)–P(1)–C(6)	114.6 (3)
C(3)–P(1)–C(6)	103.1 (4)	Rh(2)–P(2)–C(5)	115.7 (3)
Rh(2)–P(2)–C(17)	114.2 (3)	C(5)–P(2)–C(17)	102.8 (4)
Rh(2)–N(1)–C(10)	118.2 (6)	Rh(2)–N(1)–C(6A)	124.3 (6)
Rh(2)–N(2)–C(21)	118.1 (5)	Rh(2)–N(2)–C(17A)	122.8 (5)
P(1)–C(3)–C(4)	114.7 (6)	C(3)–C(4)–C(5)	112.4 (8)
P(1)–C(6)–C(7)	120.9 (7)	P(1)–C(6)–N(1A)	118.5 (6)
C(6)–C(7)–C(8)	121.9 (9)	C(7)–C(8)–C(9)	118.0 (1)
N(1)–C(10)–C(9A)	124.5 (8)	P(2)–C(17)–N(2A)	119.3 (6)
P(2)–C(17)–C(18)	120.2 (6)	C(18)–C(19)–C(20)	118.8 (9)
C(17)–C(18)–C(19)	120.2 (8)	N(2)–C(21)–C(20A)	123.4 (8)
Cl(1)–Rh(1)–C(2)	88.8 (4)	C(1)–Rh(1)–C(2)	89.3 (6)
Cl(3)–Rh(2)–N(1)	92.9 (2)	C(10)–N(1)–C(6A)	117.4 (7)
P(1)–Rh(2)–P(2)	90.55 (9)	C(21)–N(2)–C(17A)	118.4 (7)
P(1)–Rh(2)–Rh(2A)	89.52 (7)	P(2)–C(5)–C(4)	113.4 (6)
P(2)–Rh(2)–Rh(2A)	88.86 (6)	C(7)–C(6)–N(1A)	120.5 (8)
N(2)–Rh(2)–Rh(2A)	93.3 (2)	C(8)–C(9)–C(10A)	117.0 (1)
C(18)–C(17)–N(2A)	120.5 (8)	C(19)–C(20)–C(21A)	119.0 (1)

[a] Atoms labeled A are related to those in Table VI by the symmetry operation (1 – *x*, –*y*, –*z*).

solution in hexane was cooled to −40 °C, and a solution of 33 mL of 2-bromopyridine (54.6 g, 0.35 mol) in 50 mL of ether was slowly added to the stirred mixture, which was kept below −20 °C. When all bromopyridine had been added, the temperature was allowed to rise slowly to −5 °C, kept there for 5 min, and then lowered again to −35 °C. The solution of zinc chloride was then added slowly (during this addition, a sticky precipitate is formed that may hinder the stirrer; mechanical stirring is recommended), while the temperature was kept below −20 °C. After the addition was completed, the cooling bath was removed, and 200 mL of THF and 100 mL of pyridine were added. An oil, consisting mainly of $[2\text{-}C_5H_4NZnCl\cdot C_5H_5N]_2$, was formed, which solidified on standing overnight.

The next day, the solid crust was detached from the walls of the vessel and converted into a fine powder by thorough mechanical stirring. The solvent was decanted, and the solid was washed with two 300-mL portions of ethyl ether. THF (300 mL) and pyridine (100 mL) were added. In a second flask, 53 mL (69.9 g, 0.39 mol) of phenyldichlorophosphine was mixed with 100 mL of pyridine, and the mixture was cooled to −20 °C. In the course of 30 min, the suspension of pyridylzinc chloride in THF/pyridine was added in portions to the $PhPCl_2$ solution through a glass joint. After the addition, the reaction mixture was warmed to 60 °C for 30 min. The solvents were removed in vacuo, and the residue was extracted with three 250-mL portions of hexane. The hexane was evaporated, and the residue was distilled in vacuo, giving first a small forerun of $PhPCl_2$ (bp 54 °C/1 Torr) and then 38 g of PhPyPCl (bp 142 °C/1 Torr), overall yield 50%. The faintly yellow product solidified on standing.

DPyPM, DPyPE, and DPyPP. Small pieces of sodium (3.23 g, 140 mol) and ca. 20 mg of 4,4′-di-*tert*-butylbiphenyl were added to a solution of 15 g (68 mmol) of PhPyPCl in 120 mL of THF. The initially colorless mixture was refluxed until the color had changed to dark red (this may take from 1 to 14 days!) and then for an additional 24 h, at which time all the sodium had been consumed. The solution of PhPyPNa was cooled to −78 °C, and a solution of 34 mmol of methylene chloride, ethylene chloride, or propylene chloride in 25 mL of THF was added in the course of 30 min. The mixture was warmed to room temperature, most of the solvent was removed in vacuo, and 75 mL of a 4 M NaOH solution was added. The mixture was extracted with three portions of methylene chloride (125 mL, 2 × 50 mL), the solvent was stripped, and the products were purified by column chromatography (CH_2Cl_2, silica gel). DPyPM solidifies on standing, DPyPE is a white solid, and DPyPP remained an oil.

Rhodium Complexes. DPyPM[Rh(CO)Cl]$_2$ (1). A solution of 0.97 g of DPyPM (2.5 mmol) in 10 mL of THF was added dropwise to a stirred suspension of 0.98 g of $[Rh(CO)_2Cl]_2$ (2.5 mmol) in 30 mL of THF. The solution turned dark purple, and a dark precipitate slowly formed with evolution of gas. After 18 h, the supernatant was decanted, and the dark precipitate was washed with two portions of 10 mL of THF and dried in vacuo, giving a brown powder. Anal. Calcd for $C_{25}H_{20}Cl_2N_2O_2P_2Rh_2$: C, 41.78; H, 2.80; Cl, 9.87; P, 8.57. Found: C, 41.63; H, 2.81; Cl, 9.85; P, 8.52. IR (Nujol mull) 1980 (vs) cm^{-1} [ν(CO)]. The complex was recrystallized from acetonitrile to give long dark brown-red needles of this acetonitrile solvate.

$[L_2Rh_2Cl_2][Rh(CO)_2Cl_2]_2$, L = DPyPE or DPyPP (2). A solution of 1 g of DPyPE or 1.04 g of DPyPP (2.5 mmol) in 10 mL of THF was added dropwise to a stirred suspension of 0.98 g of $[Rh(CO)_2Cl]_2$ (2.5 mmol) in 30 mL of THF. The solution turned dark red-brown, and a red solid was slowly formed. After 18 h, the supernatant was decanted, and the red precipitate was washed with two portions of 10 mL of THF and dried in vacuo. The DPyPP complex was recrystallized from hot benzonitrile to give small red diamond-shaped crystals, suitable for X-ray diffraction. Anal. Calcd for $C_{54}H_{48}Cl_6N_4O_4P_4Rh_4$: C, 41.46; H, 3.09; Cl, 13.60; P, 7.87. Found: C, 41.54; H, 3.06; Cl, 13.83; P, 7.74.

IR (Nujol mull) 2062 (vs), 1982 (vs) cm^{-1} [ν(CO)].

X-ray Structure Determinations. 1. Needles of the bis(acetonitrile) solvate were dried by passing dry nitrogen over them (drying in vacuo resulted in loss of MeCN). A single crystal, suitable for X-ray diffraction, was mounted in a thin-walled glass capillary under nitrogen and held in place by an epoxy glue. All measurements were made on a Nicolet P3m diffractometer at room temperature, using graphite-monochromated Mo Kα X-radiation (λ = 0.71069 Å). Two check reflections, remeasured after every 100 ordinary data, showed 18% decay over the period of data collection, and an appropriate correction was therefore applied, as were Lorentz and polarization corrections. The intensity data were corrected for absorption effects by calculation of transmission coefficients based on a six-parameter fit to 400 azimuthal scan data. The structure was solved by conventional heavy-atom (Patterson and Fourier) methods. All non-hydrogen atoms were assigned ansitropic thermal parameters and refined without positional constraints. All hydrogens were constrained to idealized geometries (C–H = 0.96 Å; ∠H–C–H = 109.5° for aliphatic hydrogens) and assigned common isotropic temperature parameters by type (i.e., phenyl and pyridyl, methylene and methyl). The structure was refined by full-matrix blocked-cascade least-squares analysis. All calculations were carried out on a Nicolet R3m/V structure determination system using programs of the SHELXTL-PLUS package.[7] Neutral-atom scattering factors were taken from ref 8. Details of the data collection and structure determination are gathered in Table III, positional and equivalent isotropic thermal parameters are given in Table IV, and selected bond distances and angles are collected in Table V.

2. Suitable crystals were obtained by crystallization from hot benzonitrile. The structure determination was carried out as described above, with the following differences. The absorption correction was carried out numerically: crystal faces [distances from origin in mm] (101) [0.35], (010) [0.092], (0,–1,0) [0.092], (–3,–2,4) [0.075], (1,0,–1) [0.075], (–1,–1,0) [0.15], (–1,1,0) [0.13]. Three check reflections remeasured after every 50 ordinary data showed no significant variation during data collection. Nonhydrogen atoms were refined anistropically; hydrogens were constrained to idealized geometries and assigned fixed isotropic displacement parameters ca. 1.2 times U_{iso} of their attached carbon atom. Positional and equivalent isotropic thermal parameters are given in Table VI, and selected bond distances and angles are collected in Table VII.

Supplementary Material Available: Tables of positional and thermal parameters and bond lengths and angles for 1 and 2 (6 pages); tables of observed and calculated structure factors for compounds 1 and 2 (56 pages). Ordering information is given on any current masthead page.

---

[7] Sheldrick, G. M. SHELXTL-PLUS Rev. 2.2, Güttingen, F. R. G., 1987.

[8] *International Tables for X-ray Crystallography*; Kynoch Press: Birmingham, 1974; Vol. IV.

Synthesis of Dipositive Molybdenum(II) and Tungsten(II) Carbonyl Cations by Electrochemically Generated Internal Addition Reactions

Alan M. Bond,*[,1] Ray Colton,*[,2] and Katherine McGregor[2]

Department of Chemical and Analytical Sciences, Deakin University, Geelong, Victoria 3217, Australia, and Department of Inorganic Chemistry, University of Melbourne, Parkville, Victoria 3052, Australia

Received October 5, 1989

Electrochemical oxidation of $M(CO)_3(\eta^1\text{-L-L})(\eta^2\text{-L-L})$ (M = Mo, W; L-L = various ditertiary phosphines and a mixed phosphine/arsine) in acetone (0.1 M Et_4NClO_4) or in dichloromethane (0.1 M Bu_4NClO_4) solution under carbon monoxide at a platinum electrode yields isolable $[M(CO)_3(\eta^2\text{-L-L})_2]^{2+}$ cations by the electrochemically generated internal addition reaction $M(CO)_3(\eta^1\text{-L-L})(\eta^2\text{-L-L}) \rightarrow [M(CO)_3(\eta^2\text{-L-L})_2]^{2+} + 2e^-$. Electrochemical synthesis therefore provides at present the only route to novel dipositive carbonyl cations in the special case where a pendent phosphorus (or arsenic) atom is available to provide the additional donor ligand required to achieve an 18-electron configuration. Chemical oxidations do not give the same products because of nucleophilic attack by solvent, the anion of the oxidant, or adventitious impurities on the dipositive cation. The $[M(CO)_3(\eta^2\text{-L-L})_2]^{2+}$ cations decompose very slowly under carbon monoxide and much more rapidly under nitrogen to give first the 16-electron *trans*-$[M(CO)_2(\eta^2\text{-L-L})_2]^{2+}$ species (or weakly solvated species), which then undergo nucleophilic attack by the electrochemical supporting electrolyte NBu_4ClO_4 to generate $[M(CO)_2(\eta^2\text{-L-L})_2(ClO_4)]^+$: $[M(CO)_3(\eta^2\text{-L-L})_2]^{2+} \rightarrow$ *trans*-$[M(CO)_2(\eta^2\text{-L-L})_2]^{2+} \rightarrow [M(CO)_2(\eta^2\text{-L-L})_2(ClO_4)]^+$. The product of the oxidation of $Mo(CO)_3(\eta^1\text{-dpm})(\eta^2\text{-dpm})_2$ (dpm = $Ph_2PCH_2PPh_2$) by $AgClO_4$ has been isolated and shown to be $Mo(\eta^2\text{-dpm})_2(ClO_4)_2$, but its structure is not known.

Introduction

Oxidation state II molybdenum and tungsten carbonyl complexes are well-known, and they usually have seven-coordinate geometry.[3,4] They were originally prepared by halogen oxidation of substituted zerovalent carbonyl compounds[3,5] such as in eq 1. In these chemical oxidative

$$Mo(CO)_4(PPh_3)_2 + Br_2 \rightarrow Mo(CO)_3(PPh_3)_2Br_2 + CO \qquad (1)$$

reactions, the stable 18-electron configuration is retained in both the zerovalent and divalent complexes.

Electrochemical oxidation studies of zerovalent molybdenum and tungsten compounds have also been carried out. In most cases an overall two-electron oxidation is

---

[1] Deakin University.

[2] University of Melbourne.

[3] Colton, R. *Coord. Chem. Rev.* 1971, *6*, 269.

[4] Wilkinson, G., Stone, F. G. A., Abel, A. W., Eds.; *Comprehensive Organometallic Chemistry*; Pergamon Press: Oxford, England, 1982; Vol. 3, Chapter 27.

[5] Lewis, J.; Whyman, R. *J. Chem. Soc.* 1965, 5486.

0276-7333/90/2309-1227$02.50/0